

Univerza  
v Ljubljani  
Fakulteta  
*za gradbeništvo  
in geodezijo*



Jamova 2  
1000 Ljubljana, Slovenija  
<http://www3.fgg.uni-lj.si/>

**DRUGG** – Digitalni repozitorij UL FGG  
<http://drugg.fgg.uni-lj.si/>

Ta članek je avtorjeva zadnja recenzirana različica, kot je bila sprejeta po opravljeni recenziji.

Prosim, da se pri navajanju sklicujete na bibliografske podatke, kot je navedeno:

University  
of Ljubljana  
Faculty of  
*Civil and Geodetic  
Engineering*



Jamova 2  
SI – 1000 Ljubljana, Slovenia  
<http://www3.fgg.uni-lj.si/en/>

**DRUGG** – The Digital Repository  
<http://drugg.fgg.uni-lj.si/>

This version of the article is author's manuscript as accepted for publishing after the review process.

When citing, please refer to the publisher's bibliographic information as follows:

Vrankar, L., Turk, G. in Runovc, F. 2004. Combining the radial basis function Eulerian and Lagrangian schemes with geostatistics for modeling of radionuclide migration through the geosphere. *Computers & Mathematics with Applications* 48, 10–11: 1517–1529.  
DOI: 10.1016/j.camwa.2004.05.006.

# Combining the Radial Basis Function Eulerian and Lagrangian Schemes with Geostatistics for Modeling of Radionuclide Migration through the Geosphere

Leopold Vrankar

*Slovenian Nuclear Safety Administration  
Železna cesta 16, 1001 Ljubljana, Slovenia  
leopold.vrankar@gov.si*

Goran Turk

*University of Ljubljana, Faculty of Civil and Geodetic Engineering  
Jamova cesta 2, 1000 Ljubljana, Slovenia  
gturk@fgg.uni-lj.si*

Franc Runovc

*University of Ljubljana, Faculty of Natural Sciences and Engineering  
Aškerčeva 12, 1000 Ljubljana, Slovenia  
franc.runovc@uni-lj.si*

---

## Abstract

To assess the long term safety of a radioactive waste disposal system, mathematical models are used to describe groundwater flow, chemistry and potential radionuclide migration through geological formations. A number of processes need to be considered when predicting the movement of radionuclides through the geosphere. The most important input data are obtained from field measurements, which are not available for all regions of interest. For example, the hydraulic conductivity as an input parameter varies from place to place. In such cases geostatistical science offers a variety of spatial estimation procedures. Methods for solving the solute transport equation can also be classified as Eulerian, Lagrangian and mixed. The numerical solution of partial differential equations (PDE) has usually been obtained by finite difference methods (FDM), finite element methods (FEM), or finite volume methods (FVM). Kansa introduced the concept of solving partial differential equations using radial basis functions (RBF) for hyperbolic, parabolic and elliptic PDEs. The aim of this study was to present a relatively new approach to the modeling of radionuclide migration through the geosphere using radial basis function methods in Eulerian and Lagrangian coordinates. In this study we determine the average and

standard deviation of radionuclide concentration with regard to variable hydraulic conductivity which was modelled by a geostatistical approach. Radionuclide concentrations will also be calculated in heterogeneous and partly heterogeneous 2D porous media.

*Key words:* Radionuclide migration, Lagrangian method, Radial basis function, Eulerian method, Geostatistics

---

## 1. INTRODUCTION

Assessment of the release and the transport of long-lived radioactive nuclides from the repository to the biological environment is an important part of the safety analysis of repository concepts. Confidence in a model may be gained from its ability to fit dynamic laboratory and field experiments, which can differ in scale from a few centimeters to tens of meters. In this assessment, mathematical models describing the mechanisms involved in the nuclide transport from the repository to the biosphere are essential tools.

When modeling flow and contaminant transport in the geosphere, it is important to consider both internal processes (e.g. advection, dispersion, retardation) within the geosphere, and external processes associated with the near-field and the biosphere. For example, near-field processes can influence water flow and chemistry in the geosphere surrounding the disposal facility, whilst biosphere processes such as flooding, erosion, weathering, recharge and environmental change all can have an impact on the geosphere [1].

The general reliability and accuracy of transport modeling depend predominantly on input data such as hydraulic conductivity, water velocity on the boundary, radioactive inventory, hydrodynamic dispersion. The output data are concentration, pressure, etc. The most important input data are obtained from field measurement, which are not available for all regions of interest. For example, the hydraulic conductivity as an input parameter varies from place to place.

In such cases geostatistical science offers a variety of spatial estimation procedures. The term geostatistics is employed here as a generic term, meaning the application of the theory of random fields in the earth sciences [2]. The parameters are distributed in space and can be thus called regionalized variables. The parameters of a given geologic formation can conveniently be represented as realizations of random variables which form random fields.

Methods for solving the solute transport equation can also be classified as Eulerian, Lagrangian and mixed. Eulerian methods are based on discretization on fixed grid. Lagrangian methods are based on solving transport equation in a deformable grid, defined over fixed coordinates [3].

The numerical solution of partial differential equations has been usually obtained by either finite difference methods (FDM), finite element methods (FEM), finite volume methods (FVM), and boundary elements methods (BEM) [4]. These methods require a mesh to support the localized approximations. The construction of a mesh in two or more dimensions is not trivial problem. Usually, in practice, only low-order approximations are employed resulting in a continuous approximation of the function across the mesh but not its partial derivatives. The discontinuity of the approximation of the derivative can adversely effect the stability of the solution. While higher-order schemes are necessary for more accurate approximations of the spatial derivatives, they usually involve additional computational cost [5] and may also cause some numerical problems, such as locking.

A fairly new approach for solving PDEs stems from radial basis functions (RBF). In 1990, Dr. Kansa introduced the concept of solving PDEs using radial basis functions for hyperbolic, parabolic and elliptic PDEs. A key feature of an RBF method is that it does not require a grid. The only geometric properties that are used in an RBF approximation are the pairwise distances between points. Distances are easily computed in any number of spatial dimensions, thus working in higher dimensions does not increase the difficulty. Over the last 30 years, many researchers have shown a great deal of interest in RBFs. It was used for groundwater modeling [6], modeling radionuclide migration [7], solving torsion problems [8] and for many other problems [9].

The aim of this study was to focus to present a relatively new approach to modeling of radionuclide migration through the geosphere using radial basis function methods in Eulerian and Lagrangian coordinates. In this study we determine the average and standard deviation of radionuclide concentration with regard to variable hydraulic conductivity that was modelled by a geostatistical approach. Radionuclide concentrations will also be calculated in heterogeneous and partly heterogeneous porous media.

## 2. GEOSTATISTICS

Many processes are inherently uncertain, and this uncertainty is handled through the use of stochastic realizations. The goal of stochastic simulation is

to reproduce geological texture in a set of equiprobable simulated realizations. In mathematical terms, the most convenient method for simulation is sequential Gaussian simulation because all successive conditional distributions from which simulated values are drawn are Gaussian with parameters determined by the solution of a simple kriging system.

Sequential Gaussian simulation procedure [10]:

- (1) First, use a sequential Gaussian simulation to transform the data into a normal distribution.
- (2) Then performs variogram modelling on the data. Select one grid node at random, then kriging the value at that location. This will also give us the kriged variance.
- (3) Then draw a random number from a normal distribution that has a variance equivalent to the kriged variance and a mean equivalent to the kriged value. This number will be the simulated number for that grid node.
- (4) Select another grid node at random and repeat. For the kriging, include all the previously simulated nodes to preserve the spatial variability as modelled in the variogram.
- (5) When all nodes have been simulated, back transform to the original distribution. This gives us first realization using a different random number sequence to generate multiple realizations of the map.

Kriging (named after D. G. Krige, a South African mining engineer and pioneer in the application of statistical techniques to mine evaluation) is a collection of generalized linear regression techniques for minimizing an estimation variance defined from a prior model for a covariance (semivariogram) [10].

### 3. RADIAL BASIS FUNCTIONS

A radial basis function is a function  $\phi_j(\mathbf{x}) = \phi(\|\mathbf{x} - \mathbf{x}_j\|)$ , which depends only on the distance between  $\mathbf{x} \in \mathbf{R}^d$  and a fixed point  $\mathbf{x}_j \in \mathbf{R}^d$ . Here,  $\phi$  is continuous and bounded on any bounded sub-domain  $\Omega \subseteq \mathbf{R}^d$ . Let  $r$  denote by the Euclidean distance between any pair of points in the domain  $\Omega$ .

The commonly used radial basis functions are:

$\phi(r) = r,$	linear,
$\phi(r) = r^3,$	cubic,
$\phi(r) = r^2 \log r,$	thin-plate spline,
$\phi(r) = e^{-\alpha r^2},$	Gaussian,
$\phi(r) = (r^2 + c^2)^{\frac{1}{2}},$	multiquadric,
$\phi(r) = (r^2 + c^2)^{-\frac{1}{2}},$	inverse multiquadric,

In our case we used multiquadric (MQ) and inverse multiquadric radial basis functions. MQ method was first introduced by Hardy [11]. The parameter  $c > 0$  is a positive shape parameter controlling the fitting of a smoothing surface to the data.

Since Kansa [12], [13] successfully modified the radial basis functions for solving PDEs of elliptic, parabolic, and hyperbolic types, more and more computational tests showed that this method is feasible for solving various PDEs.

To introduce RBF collocation methods, we consider a PDE in the form of

$$L u = f(\mathbf{x}) \quad \text{in } \Omega \subset \mathbf{R}^d, \quad (1)$$

$$B u = g(\mathbf{x}) \quad \text{on } \partial\Omega, \quad (2)$$

where  $d$  is the dimension,  $\partial\Omega$  denotes the boundary of the domain  $\Omega$ ,  $L$  is the differential operator on the interior, and  $B$  is an operator that specifies the boundary conditions of the Dirichlet, Neumann or mixed type. Both,  $f$  and  $g$ , are given functions mapping  $\mathbf{R}^d \rightarrow \mathbf{R}$ .

Using Kansa's asymmetric multiquadric collocation method, the unknown PDE solution  $u$  is approximated by RBFs in the form

$$u \approx U(\mathbf{x}) = \sum_{j=1}^N \alpha_j \phi_j(\mathbf{x}) + \sum_{l=1}^M \gamma_l v_l(\mathbf{x}), \quad (3)$$

where  $\phi_j(\mathbf{x}) = \phi(\|\mathbf{x} - \mathbf{x}_j\|)$ , and  $\phi$  can be any radial basis function from the list,  $v_1, \dots, v_M \in \Pi_m^d$  is a polynomial of degree  $m$  or less,  $M := \binom{m-1+d}{d}$  [14] and  $\|\cdot\|$  indicates the Euclidean norm. Let  $\{(\mathbf{x}_j, u_j)\}_{j=1}^N$  be the  $N$  collocation points in  $\Omega \cup \partial\Omega$ . We assume the collocation points are arranged in such a way

that the first  $N_I$  points are in  $\Omega$ , whereas the last  $N_B$  points are on  $\partial\Omega$ . To solve for the  $N + M$  unknown coefficients,  $N + M$  linearly independent equations are needed. Ensuring that  $U(\mathbf{x})$  satisfies (1) and (2) at the collocation points results in a good approximation of the solution  $u$ . The first  $N$  equations are given by

$$\begin{aligned} \sum_{j=1}^N \alpha_j L \phi_j(\mathbf{x}_i) &= f(\mathbf{x}_i) \quad \text{for } i = 1, \dots, N_I \\ \sum_{j=1}^N \alpha_j B \phi_j(\mathbf{x}_i) &= g(\mathbf{x}_i) \quad \text{for } i = N_I + 1, \dots, N_I + N_B \end{aligned} \quad (4)$$

The last  $M$  equations could be obtained by imposing some extra condition on  $v(\cdot)$ :

$$\sum_{j=1}^N \alpha_j v_k(\mathbf{x}_j) = 0, \quad k = 1, \dots, M. \quad (5)$$

In many practical applications (in the case of MQ), it is observed that the term  $\sum_{l=1}^M \gamma_l v_l(\mathbf{x})$  does not have great effect on the accuracy of the method [14].

## 4. MODELING OF THE RADIONUCLIDE MIGRATION

The safe handling and disposal of radioactive wastes is a prerequisite for the exploitation of nuclear power. Extensive research and development in the field of management and disposal of radioactive waste is conducted in many countries. To a large extent this work is directed towards finding methods for disposal of high-level waste. In the evaluation of the final disposal of radioactive waste in deep geological media it is necessary to obtain adequate data on the characteristics of possible sites and different repository designs. It is also essential to apply appropriate tools for the evaluation of the safety of the entire disposal system.

Assessment of the release and the transport of long-lived radioactive nuclides from the repository to the biological environment is an important part of the safety analysis of repository concepts. In this assessment mathematical models describing the mechanisms involved in the nuclide transport from the repository to the biosphere are essential tools. For example, the groundwater models are mathematical representations of the flow of the water and the transport of solutes in the subsurface. Models are used to compute the hydraulic head,

velocity, concentration, etc., from hydrologic and mass inputs, hydrogeologic and mass-transfer parameters, and conditions at the boundary of the domain.

The numerical methods are developed both with regard to efficiency and ability to solve a wider variety of problems. A high efficiency is necessary to be able to solve physically complicated problems in two or three dimensions. The most common present methods like finite difference, finite element, etc., often suffer the drawback that they require fine discretisations to solve predominantly advective problems. In the conclusions of INTRACOIN project [15] it was reported that there are two complementary lines of development in the field of radionuclide transport modeling. The first is towards more sophisticated and detailed models for deterministic analyses and the second towards simpler models for probabilistic analyses.

Groundwater models are presented by motion and continuity equations. The majority of the codes currently used or under development are based on the advective-dispersive equation [16] with various physical phenomena added. According to this equation, mass transport is controlled by two mechanisms: advection and dispersion. Advection accounts for the movement of the solute, linked to the fluid, with the average water velocity. Water velocity can be assessed through Darcy's law. Dispersion accounts for mixing caused by diffusion and by random departures from the mean stream.

#### 4.1 Laplace equation

The first step of radionuclide transport modeling is to solve the Laplace equation to obtain the Darcy velocity. In this case the Neumann and Dirichlet boundary conditions will be defined along the boundary. Homogeneous and anisotropic porous media and incompressible fluid are assumed. The equation has the following form [16]:

$$K_x \frac{\partial^2 p}{\partial x^2} + K_z \frac{\partial^2 p}{\partial z^2} = 0, \quad (6)$$

where  $p$  is the pressure of the fluid and  $K_x$  and  $K_z$  are the components of hydraulic conductivity tensor. The corresponding boundary conditions are:

$$\frac{\partial p}{\partial x} s_x + \frac{\partial p}{\partial z} s_z = g_1(x, z), \quad (7)$$

or

$$p = g_2(x, z). \quad (8)$$



where  $s_x$  and  $s_z$  are the components of the unit vector normal to the boundary.

The Laplace equation was solved by using direct collocation [17]. We add an additional set of nodes (outside of the domain) adjacent to the boundary and add an additional set of collocation equations. The approximate solution is expressed as :

$$p(x, z) = \sum_{j=1}^{N_I+2N_B} \alpha_j \varphi_j(x, z) \quad (9)$$

where  $\alpha_j, j = 1, \dots, N_I + 2N_B$  are the unknown coefficients to be determined and  $\varphi_j(x, z) = \sqrt{(x - x_j)^2 + (z - z_j)^2 + c^2}$  is the Hardy's multiquadrics function. By substituting (9) into (6), (7), (8), we have:

$$\sum_{j=1}^{N_I+2N_B} \left( K_x \frac{\partial^2 \varphi_j}{\partial x^2} + K_z \frac{\partial^2 \varphi_j}{\partial z^2} \right) \Big|_{x_i, z_i} \alpha_j = 0, \quad i = 1, 2, \dots, N_I + N_B, \quad (10)$$

$$\sum_{j=1}^{N_I+2N_B} \left( \frac{\partial \varphi_j(x_i, z_i)}{\partial x} s_x + \frac{\partial \varphi_j(x_i, z_i)}{\partial z} s_z \right) \alpha_j = g_1(x_i, z_i), \quad i = N_I+1, \dots, N_I+N_B, \quad (11)$$

or

$$\sum_{j=1}^{N_I+2N_B} \varphi_j(x_i, z_i) \alpha_j = g_2(x_i, z_i), \quad i = N_I + 1, \dots, N_I + N_B. \quad (12)$$

The pressure gradient is evaluated by:

$$\frac{\partial p}{\partial x} = \sum_{j=1}^{N_I+2N_B} \alpha_j \frac{\partial \varphi_j(x, z)}{\partial x}, \quad \frac{\partial p}{\partial z} = \sum_{j=1}^{N_I+2N_B} \alpha_j \frac{\partial \varphi_j(x, z)}{\partial z}. \quad (13)$$

For the calculation of velocity in principal directions we use Darcy's law [16]:

$$v_x = - \left( \frac{K_x}{\omega \rho a} \right) \frac{\partial p}{\partial x}, \quad v_z = - \left( \frac{K_z}{\omega \rho a} \right) \left( \frac{\partial p}{\partial z} \right). \quad (14)$$

where  $\rho$  is the density of the fluid,  $\omega$  is porosity and  $a$  is gravitational acceleration.

## 4.2 Eulerian Form of the Advection-Dispersion Equation

In the next step, the velocities obtained from Laplace equation are used in the advection-dispersion equation. The advection-dispersion equation for trans-

port through the saturated porous media zone at a macroscopic level with retardation and decay is [16]:

$$\begin{aligned}
R \frac{\partial u}{\partial t} &= \left( \frac{D_x}{\omega} \frac{\partial^2 u}{\partial x^2} + \frac{D_z}{\omega} \frac{\partial^2 u}{\partial z^2} \right) - v_x \frac{\partial u}{\partial x} - R\lambda u, & (x, z) \in \Omega, \quad 0 \leq t \leq T, \\
u|_{(x,z) \in \partial\Omega} &= g(x, z, t), & 0 \leq t \leq T \\
u|_{t=0} &= h(x, z), & (x, z) \in \Omega,
\end{aligned} \tag{15}$$

where  $x$  is the Eulerian groundwater flow axis and  $z$  is the Eulerian transverse axis in the 2D problem,  $u$  is the concentration of contaminant in the groundwater [Bqm<sup>-3</sup>],  $D_x$  and  $D_z$  are the components of dispersion tensor [m<sup>2</sup>y<sup>-1</sup>] in saturated zone,  $\omega$  is porosity of the saturated zone [-],  $v_x$  is Darcy velocity [my<sup>-1</sup>] at interior points,  $R$  is the retardation factor in the saturated zone [-] and  $\lambda$  is the radioactive decay constant [y<sup>-1</sup>]. In these cases [y] means years.

For the parabolic problem, we consider the implicit scheme:

$$R \frac{u^{n+1} - u^n}{\delta t} = \left( \frac{D_x}{\omega} \frac{\partial^2 u^{n+1}}{\partial x^2} + \frac{D_z}{\omega} \frac{\partial^2 u^{n+1}}{\partial z^2} \right) - v_x \frac{\partial u^{n+1}}{\partial x} - R\lambda u^{n+1}, \tag{16}$$

where  $\delta t$  is the time step and  $u^n$  and  $u^{n+1}$  are the contaminant concentrations at the time  $t_n$  and  $t_{n+1}$ . The approximate solution is expressed as :

$$u(x, z, t_{n+1}) = \sum_{j=1}^N \alpha_j^{n+1} \varphi_j(x, z) \tag{17}$$

where  $\alpha_j^{n+1}$ ,  $j = 1, \dots, N$  are the unknown coefficients to be determined and  $\varphi_j(x, z) = \sqrt{(x - x_j)^2 + (z - z_j)^2 + c^2}$  is Hardy's multiquadrics function.

By substituting (17) into (15), we obtain:

$$\begin{aligned}
\sum_{j=1}^N \left( R \frac{\varphi_j}{\delta t} - \frac{D_x}{\omega} \frac{\partial^2 \varphi_j}{\partial x^2} - \frac{D_z}{\omega} \frac{\partial^2 \varphi_j}{\partial z^2} + v_x \frac{\partial \varphi_j}{\partial x} + R\lambda \varphi_j \right) \Big|_{x_i, z_i} \alpha_j^{n+1} &= \\
&= R \frac{u^n(x_i, z_i)}{\delta t}, \quad i = 1, 2, \dots, N_I
\end{aligned} \tag{18}$$

$$\sum_{j=1}^N \varphi_j(x_i, z_i) \alpha_j^{n+1} = g(x_i, z_i, t_{n+1}), \quad i = N_I + 1, N. \tag{19}$$

The system of linear equations ((18)-(19)) for the unknown  $\alpha_j^{n+1}$ ,  $j = 1, \dots, N$  has to be solved, where  $N = N_I + N_B$  be the number of collocation points,  $N_I$  is the number of interior points and  $N_B$  is the number of boundary points. Equation (17) gives the approximate solution at any point in the domain  $\Omega$ .

### 4.3 Lagrangian Form of the Advection-Dispersion Equation

In this case the time-derivative term and the advection term of equation (15) are expressed as a material derivative:

$$\frac{du}{dt} \equiv \frac{\partial u}{\partial t} + \mathbf{v} \cdot \nabla u \quad (20)$$

After including the material derivative into the advection-dispersion equation (the second summand in  $\mathbf{v} \cdot \nabla u$  vanishes because it was assumed that  $\mathbf{v}$  is a vector with components  $v_x$  and  $v_z$ ), we have:

$$\frac{du}{dt} = \left( \frac{D_x}{R\omega} \frac{\partial^2 u}{\partial x^2} + \frac{D_z}{R\omega} \frac{\partial^2 u}{\partial z^2} \right) - \lambda u \quad (21)$$

The material derivative is approximated by:

$$\frac{du}{dt} \cong \frac{u^{n+1}(x_L^{n+1}, z_L^{n+1}) - u^n(x_L^n, z_L^n)}{\delta t} \quad (22)$$

where  $\delta t$  is the time step and  $u^n$  and  $u^{n+1}$  are the contaminant concentrations at the time  $t_n$  and  $t_{n+1}$ . Then  $x_L^{n+1}$  and  $z_L^{n+1}$  are Lagrangian coordinates:

$$\begin{aligned} x_L^{n+1} &= x_L^n + \frac{v(x_L^n, z_L^n)}{R} \delta t \\ z_L^{n+1} &= z_L^n + \frac{v(x_L^n, z_L^n)}{R} \delta t \end{aligned} \quad (23)$$

Thus, the equation (21) has the following form:

$$\begin{aligned} &\frac{u^{n+1}(x_L^{n+1}, z_L^{n+1}) - u^n(x_L^n, z_L^n)}{\delta t} = \\ &= \left( \frac{D_x}{R\omega} \frac{\partial^2 u^{n+1}(x_L^{n+1}, z_L^{n+1})}{\partial x^2} + \frac{D_z}{R\omega} \frac{\partial^2 u^{n+1}(x_L^{n+1}, z_L^{n+1})}{\partial z^2} \right) - \\ &- \lambda u^{n+1}(x_L^{n+1}, z_L^{n+1}). \end{aligned} \quad (24)$$

where  $D_x = a_x v(x_L^{n+1}, z_L^{n+1})$  and  $D_z = a_z v(x_L^{n+1}, z_L^{n+1})$ ,  $a_x$  is longitudinal dispersivity,  $a_z$  transversal dispersivity [m],  $v(x_L^{n+1}, z_L^{n+1})$  is Darcy's velocity.

Formulation of equation (24) into RBFs form is similar as it is presented in subsection 4.2.

It is possible to rearrange equation (21) into the following form:

$$\frac{du}{dt} + \lambda u = \left( \frac{D_x}{R\omega} \frac{\partial^2 u}{\partial x^2} + \frac{D_z}{R\omega} \frac{\partial^2 u}{\partial z^2} \right). \quad (25)$$

The solution of non-homogeneous ordinary differential equations (ODEs) can be found as a superposition of homogeneous and particular solutions. The particular solution of ODEs was found by the method of constant modification. In our case it was assumed that  $\lambda$  (the radioactive decay constant) is constant in each time step. The solution of equation (25) is:

$$u^{n+1} = u^n \exp(-\lambda dt) + \frac{1}{2}(G^n + G^{n+1}) dt \quad (26)$$

where  $G^n$  and  $G^{n+1}$  present the right side of equation (25) at the times  $t_n$  and  $t_{n+1}$ . Derivatives  $G^n$  and  $G^{n+1}$  are actually functions of Lagrangian points which depend on time steps  $t \rightarrow t + \delta t$ .

We also use the RBF method to approximate derivatives. First, function  $u$  is approximated by:

$$u(x, z) \cong \sum_{j=1}^N \alpha_j \varphi_j(x, z) \quad (27)$$

where  $\alpha_j, j = 1, \dots, N$  are the unknown coefficients to be determined.

Assume that all points  $(x_j, z_j)$  are distinct, and denote  $u_j = u(x_j, z_j), j = 1, 2, \dots, N$ . It is required that the approximating function (27) satisfies the conditions

$$u(x_i, z_i) = u_i, \quad i = 1, 2, \dots, N \quad (28)$$

By substituting (27) into (28), we have:

$$\sum_{j=1}^N \varphi_j(x_i, z_i) \alpha_j = u_i, \quad i = 1, 2, \dots, N \quad (29)$$

The system of linear equations (29) for the unknown  $\alpha_j, j = 1, \dots, N$  has to be solved. The second derivatives are evaluated by:

$$\frac{\partial^2 u}{\partial x^2} = \sum_{j=1}^N \alpha_j \frac{\partial^2 \varphi_j(x, z)}{\partial x^2}, \quad \frac{\partial^2 u}{\partial z^2} = \sum_{j=1}^N \alpha_j \frac{\partial^2 \varphi_j(x, z)}{\partial z^2}. \quad (30)$$

## 5. NUMERICAL EXAMPLE

The simulation was implemented for a rectangular area which was 600 m long and 300 m wide. The source (initial condition) was Thorium ( $Th - 230$ ) with activity  $1 \cdot 10^6 Bq$  and half life of 77000 years. The location of the radioactive source is presented in Fig. 1. (symbol  $\diamond$  in Fig. 1).

The groundwater flow field is presented for steady-state conditions. Except for the inflow (left side) and outflow (right side), all boundaries have a no-flow condition  $\frac{\partial p}{\partial s} = 0$  ( $s$  is normal to the boundary). The inflow rate was 1 m/y. At the outflow side, time-constant pressures at the boundaries were set. Longitudinal dispersivity  $a_x$  is 200 m and transversal dispersivity  $a_z$  is 2 m. For the porosity  $\omega$  we used values between 0.25 and 0.26. The retardation constant  $R$  is 800.

It is also important to mention that kriging and RBF (multiquadric) methods are very closely related. Both multiquadric and kriging methods are interpolation schemes that fit data points of the observed values. The multiquadric method is physically deterministic, while kriging involves a stochastic process based on the theory of regionalized variables [11]. The Kriging method includes preprocessing procedures for computing discrete semivariograms and models leading to continuity, while the multiquadric uses a predetermined kernel function, the distance. The kernel function of the kriging method was obtained by fitting the proper mathematical functions to the semivariogram. Thus an important difference between multiquadric and kriging is that the choice of semivariogram is based on the computation of a discrete semivariogram sequence termed experimental semivariogram. After the semivariogram is computed, an analytical function resembling the semivariogram is usually chosen as the kernel. The shape of the experimental semivariogram in the kriging method depends upon the choice of interval and the scale of observation rather than the real unknown spatial structure of the phenomenon itself. The kriging method has a preprocessing step that is based mainly on the experience and judgement of the researcher. An exact fit of covariance with a single analytical kernel is difficult to obtain. An analytical semivariogram is frequently selected by means of least squares. In the multiquadric approach, this preliminary procedure is not relevant. In most interpolation algorithms, including kriging, the goal is to provide the best, hence unique, local estimate of the variable without specific regard to the resulting spatial statistics of the estimates taken together. For this reasons we choose a sequential Gaussian simulation which provides alternative global representation, where reproduc-

tion of patterns of spatial continuity prevails.

The distribution of hydraulic conductivity for one specific simulation is shown in Fig. 1. In Fig. 1 we cannot see a lot of variability of hydraulic conductivity. One of the reasons could be that there are not many differences between the prescribed values of hydraulic conductivity. Based on a set of prescribed values (values are: 66.00, 71.00, 73.00, 75.00, 76.52, 77.02, 79.74, 83.41 [ $\frac{m}{y}$ ]) hydraulic conductivity was generated in different points with a sequential Gaussian simulation procedure which is presented in chapter two. The coordinates of these points are also presented in Fig. 1. The following variogram parameters are chosen: positive variance contribution or sill is equal 1.0 and nugget effect is 0.0. Simple kriging is chosen as the type of kriging. A spherical model is chosen as a type of variogram structure. The angles defining the geometric anisotropy: the maximum horizontal range is 600 m and the minimum horizontal range is 300 m. It is assumed that the mean in the case of simple kriging is known. In Fig. 2 we present velocity vector. We can see that the length of the velocity is greatly dependent on hydraulic conductivity and porosity.

The distribution of the average value and standard deviation of contaminant concentration after 100,000 years are given in Fig. 3 and 4. These values were obtained after completing 100 simulations. The scatter of the results is not large, which is also indicated in Fig. 4. In nature, the hydrologic and environment variables change from location to location in complex and inadequately understood ways. In most applications, we have relied on the data to guide us in developing an empirical model. The model involves the concept of probability in the sense that spatial variability is described coarsely by using averages. In practice, our objective is to estimate a field variable  $z(\mathbf{x})$  over a region. Usually, because of scarcity of information, we cannot find a unique solution. It is useful to think of the actual unknown  $z(\mathbf{x})$  as one of a collection of possibilities  $z(\mathbf{x}; 1), z(\mathbf{x}; 2), \dots$ . This collection (ensemble) defines all possible solutions to our estimation problem. The ensemble of realizations with their probabilities defines what is known as the spatial stochastic process. We used the averaging process since specifying all possible solutions and their probabilities is not an easy task, and it is more convenient to specify and to work with ensemble averages or statistical moments (mean and covariance function). The quality of the results also depends on the quality of input data. An important measure of the spread in the data set is the mean square difference from the arithmetic mean. Its square root is the standard deviation (Fig. 4)

The calculation of the radioactive concentrations in partly heterogeneous porous media was also carried out. The results of radioactive concentrations for one particular simulation in partly heterogeneous porous media for the Eulerian and Lagrangian method are presented in Figs. 5 and 6. The results of radioactive concentrations for one particular simulation in heterogeneous porous media for the Lagrangian and Eulerian methods are presented in Figs. 7 and 8.

As known the Lagrangian method is suitable for fluid and contaminants that move. In our case the subsurface (boundary area) was fixed. There are two coordinate systems: one which is fixed involving the subsurface  $(x, z)$ , and the other moving with water and contaminants,  $(x_L, z_L)$ .

Comparison of concentrations calculated with Eulerian and Lagrangian method in partly heterogeneous porous (Fig. 5 and Fig. 6) shows that the Lagrangian methods gives us wider a concentration cloud in the area of high conductivity. It seems that it shows the influence of non-smooth change between low and high conductivity. In the case of a comparison of concentrations calculated with the Eulerian and Lagrangian method in heterogeneous porous media (Fig. 7 and Fig. 8), we can see that concentration contours calculated with Lagrangian methods are less smooth. A comparison of results in partly heterogeneous (Fig. 5 and Fig. 6) and heterogeneous (Fig. 7 and Fig. 8) porous media show that both the Lagrangian and Eulerian methods give us longer concentration clouds in partly heterogeneous porous media. The results also looks symmetrical. The reason for this is that we used a symmetrical set of boundary conditions.

The differences between the Lagrangian and Eulerian methods which we noticed in partly heterogeneous porous media (Fig. 5 and Fig. 6) were actually lost in heterogeneous porous media (Fig. 7 and Fig. 8). In partly heterogeneous porous media the hydraulic conductivity was prescribed at all points. But in the case of heterogeneous porous media we model the hydraulic conductivity as a random field with a mean and covariance function. We choose a spherical model as a type of variogram structure and simple kriging as the type of kriging. These two parameters are important input data for the sequential Gaussian simulation procedure which serves as a tool for estimating unknown hydraulic conductivity. The reason for smearing the differences between the methods could be smoothing effect of kriging.

The results of concentrations for one particular simulation in heterogeneous porous media obtained with FDM (Fig. 9) are obtained with the Eulerian approach. For the purpose of comparing FDM and the Kansa method we plotted differences (Fig. 10). The so-called normalized error was defined symbolically as:

$$\frac{|u_{FDM} - u_{RBF}|}{\max(u_{FDM}, u_{RBF})}$$

where  $u_{FDM}$  is the value calculated with FDM and  $u_{RBF}$  is the value calculated with RBF.

## 6. CONCLUSION

This work presents modeling of radionuclide migration through the geosphere using a combination of radial basis function methods in Eulerian and Lagrangian coordinates with geostatistics. In the case of radionuclide migration two steps of evaluations were performed. In the first step the velocities were determined from the pressure of the fluid  $p$  by solving the Laplace differential equation. In the second step the advection-dispersion equation was solved to find the concentration of the contaminant. In this study the Lagrangian method served as a comparative tool for an Eulerian type radial basis function method.

In practice, our objective is to estimate contaminant concentrations over a region. Usually, because of scarcity of information, we cannot find a unique solution. We are interested in calculating averages over many possible realizations. Comparison of the results between the average of contaminant concentrations (Fig. 3) and concentrations for one particular simulation (Fig. 8) shows that the more realizations we have, the more accurate are the results. The results are also very similar to the results obtained by finite difference method (Fig. 9).

Comparison of the results between Lagrangian and Eulerian method in heterogeneous porous media shows similar results. The drawback of the Lagrangian method (24) is that an estimate of the running time for the calculations of concentrations through 100,000 years was up to 600 times longer than Eulerian method, namely the number of Lagrangian steps is influenced by the time interval,  $\delta t$  (e. g. 1 year). We have to calculate a meshless matrix in each time interval, whereas in the Eulerian method the matrix is determined only once. On the other hand, the Lagrangian scheme enables us to solve simpler PDEs (25) and it is also easy to implement in RBF form. The normalized error is generally low (below 5 %) with the exception of the region with higher concentration (Fig. 10). Because the radial basis functions are truly meshfree, the Lagrangian RBF scheme does not need the remeshing that is common with Lagrangian finite difference, finite element, or finite volume schemes.

In the case of calculating the advection-dispersion equation we can conclude that the Kansa method could be an appropriate alternative to the FDM due to its simpler implementation. In general, the Eulerian approach is more convenient and is more frequently used. But if it is important to study sharp changes (in our case between areas of low and high conductivity) of the solutions where important chemistry and physics take place, it is better to use the Lagrangian RBF scheme.

**Acknowledgements** - The authors would like to thank the Slovenian Nuclear Safety Administration for their support and understanding.



## References

1. Validation of Geosphere Flow and Transport Models (GEOVAL), Proceedings of a NEA/SKI Symposium, Stockholm, May (1990).
2. P. K. Kitanidis and E. G. VoMvoris, A Geostatistical Approach to the Inverse Problem in Groundwater Modelling (Steady State) and One-Dimensional Simulations, *Water Resources Research* 19 (3), 677-690, (1983).
3. O. Cirpka, E. Frind and R. Helmig, Numerical methods for reactive transport on rectangular and streamline-oriented grids, *Advances in Water Resources* 22 (7), 711-728, (1999).
4. G. D. Smith, *Numerical Solution of Partial Differential Equations: Finite Difference Methods*, Second Edition, Oxford University Press (1978).
5. H. Power and V. Barrac, A comparison analysis between unsymmetric and symmetric radial basis function collocation methods for the numerical solution of partial differential equations, *Computers Math. Applic.* 43, 551-583, (2002).
6. Jichun Li, C. S. Chen, Darrell Pepper and Yitung Chen, Mesh-free method for groundwater modeling, Private communication.
7. L. Vrankar, G. Turk and F. Runovc, The influence of geostatistical data on the reliability of the meshless method in transport modeling, Proceedings of the International Conference Uranium Mining and Hydrogeology III and the International Mine Water Association Symposium, (Edited by B. J. Merkel, B. Planer-Friedrich and C. Wolkersdorfer), pp. 359-368, Freiberg, Germany (2002).
8. L. Vrankar, G. Turk and F. Runovc, Solving pure torsion problem and modelling radionuclide migration using radial basis functions, International Workshop on Meshfree Methods, Book of abstracts, (Edited by Carlos J. S. Alves (Instituto Superior Técnico, Portugal), C. S. Chen (University of Nevada at Las Vegas, U. S. A.), Vitor M. A. Leitão (Instituto Superior Técnico, Portugal)), pp. 125-130 (2003).
9. L. Ling, Radial basis functions in scientific computing, Ph. D. Thesis, Department of Mathematics, Simon Fraser University, Canada (2003).
10. C. V. Deutsch and A. G. Journel, *GSLIB Geostatistical Software Library and User's Guide*, Oxford University Press (1998).
11. R. L. Hardy, Multiquadric equation of topography and other irregular surfaces, *J. Geophys. Res.* 76 (26), 1905-1915, (1971).
12. E. J. Kansa, Multiquadrics—A scattered data approximation scheme with applications to computational fluid dynamics-I. Surface approximations and partial derivative estimates, *Computers Math. Applic.* 19 (8/9), 127-145, (1990).
13. E. J. Kansa, Multiquadrics—A Scattered data approximation scheme with applications to computational fluid dynamics-II. Solutions to parabolic,

- hyperbolic and elliptic partial differential equations, *Computers Math. Applic.* 19 (8/9), 147-161, (1990).
14. Mao Xian Zhong, Radial basis function method for solving differential equations, Ph. D. Thesis, Department of Mathematics, City University of Hong Kong, School of Graduate Studies, Chine (1999).
  15. INTRACOIN, International Nuclide Transport Code, Intercomparison Study, SKI, May (1986).
  16. J. Bear and A. Verruijt, *Modeling Groundwater Flow and Pollution*, D. Reidel Publishing Company, Dordrecht, Holland (1987).
  17. A. I. Fedoseyev, M. J. Friedman and E. J. Kansa, Improved multiquadric method for elliptic partial differential equations via PDE collocation on the boundary, *Computers Math. Applic.* 43, 439-455, (2002).

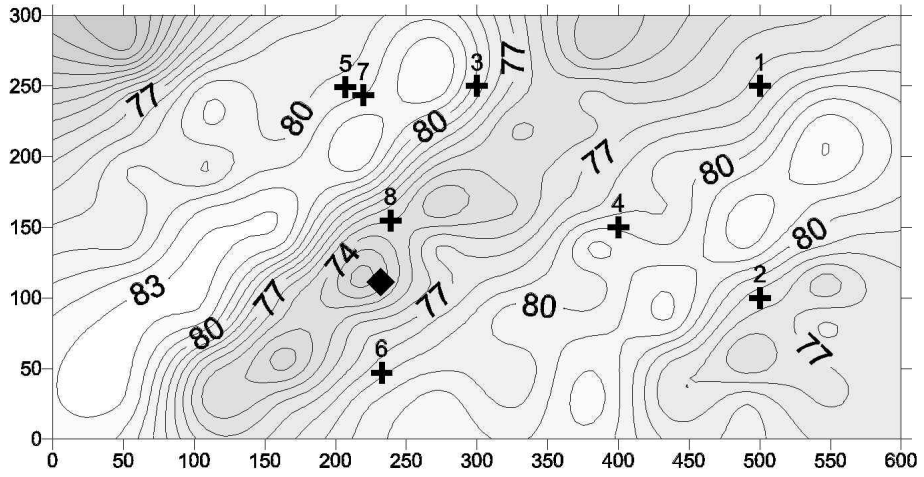


Fig. 1: Distribution of hydraulic conductivity based on an 8-point data set

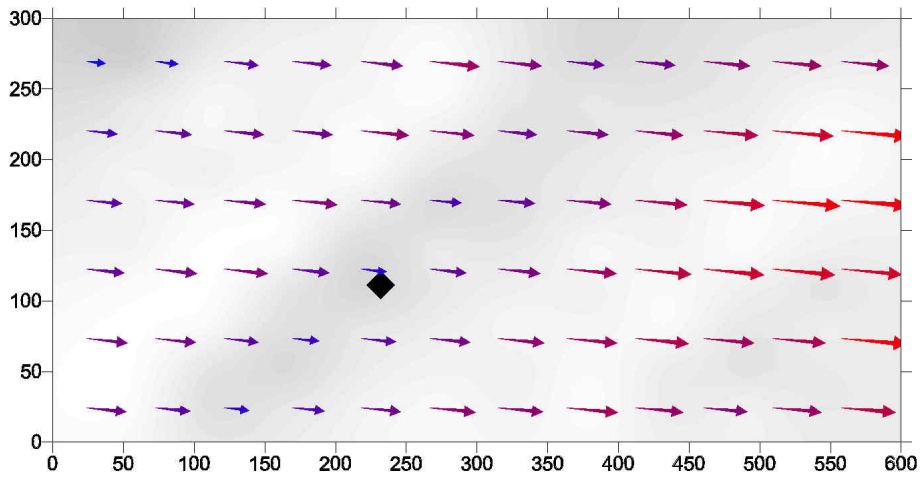


Fig. 2: Calculated Darcy's velocity (Eulerian method)

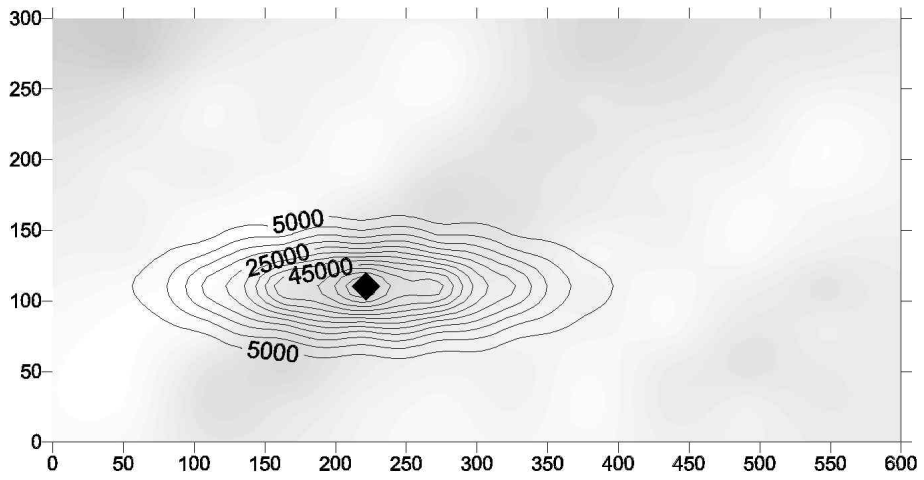


Fig. 3: Average of contaminant concentrations in heterogeneous porous media (Eulerian method)

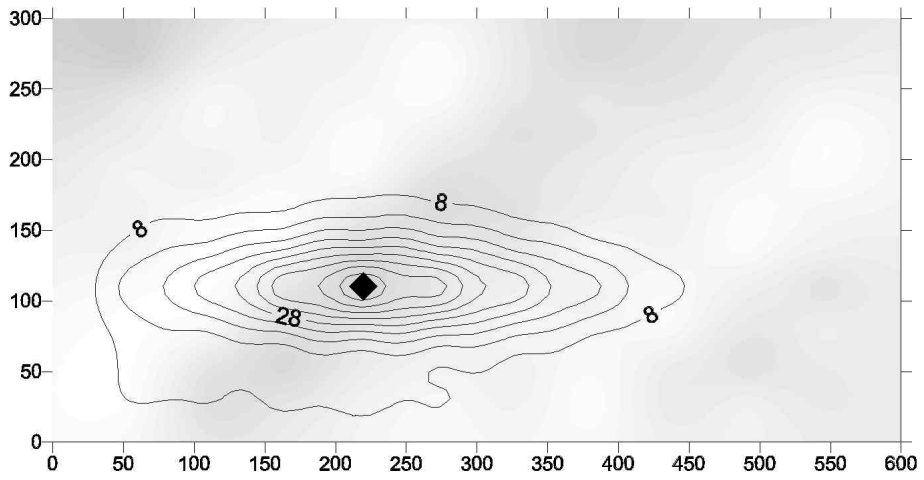


Fig. 4: Standard deviation of contaminant concentrations in heterogeneous porous media (Eulerian method)

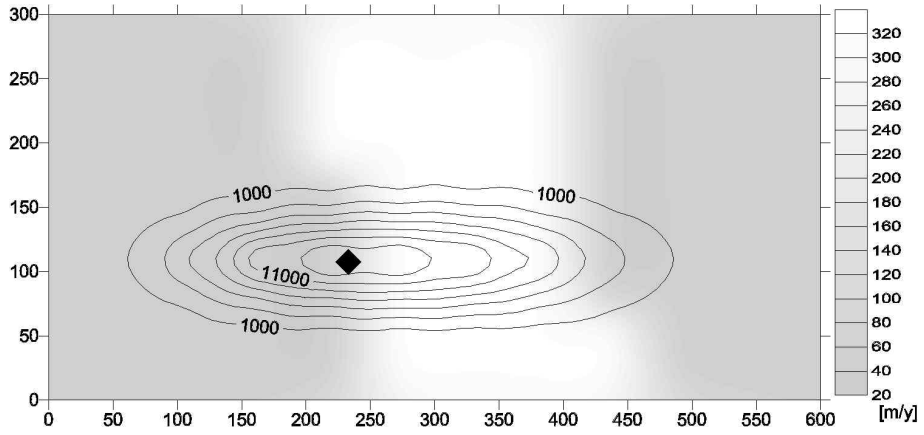


Fig. 5: Concentrations and Conductivity in partly heterogeneous porous media size 50 and 320 [ $\frac{m}{y}$ ] (Eulerian method)

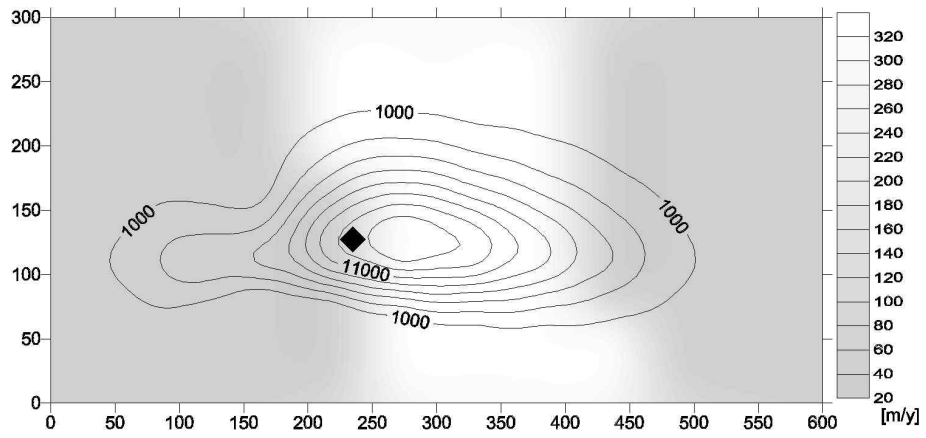


Fig. 6: Concentrations and Conductivity in partly heterogeneous porous media size 50 and 320  $[\frac{m}{y}]$  (Lagrangian method)



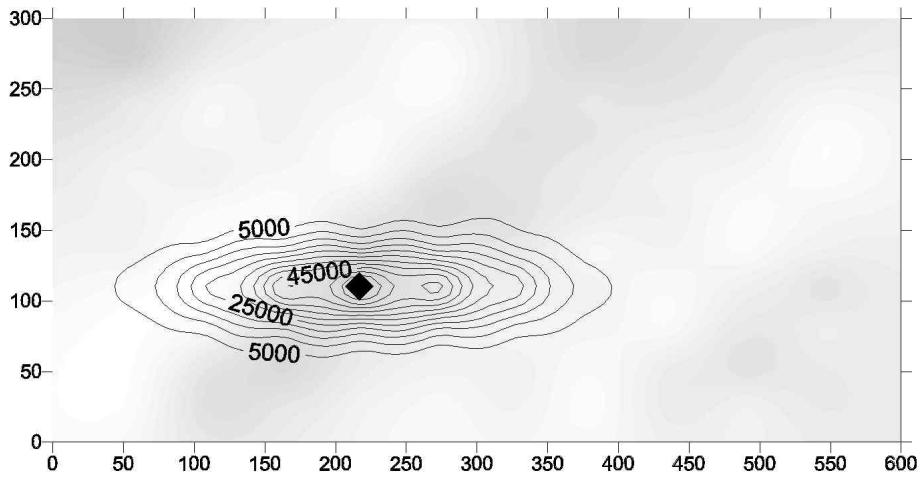


Fig. 7: Concentrations in heterogeneous porous media for one particular simulation (Lagrangian method)

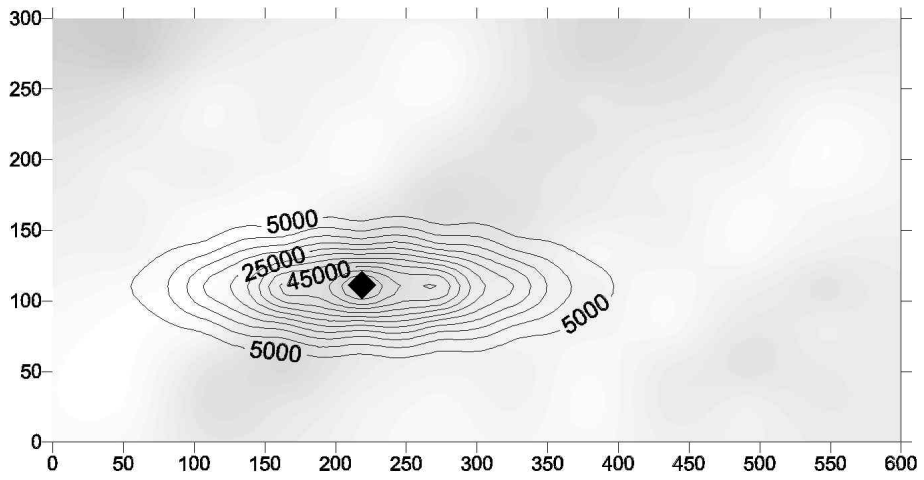


Fig. 8: Concentrations in heterogeneous porous media for one particular simulation (Eulerian method)

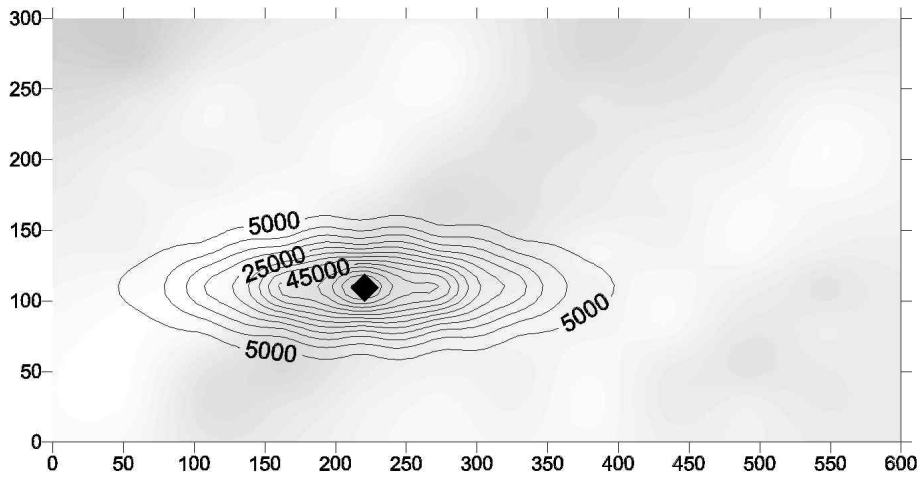


Fig. 9: Concentrations in heterogeneous porous media for one particular simulation (finite difference method)

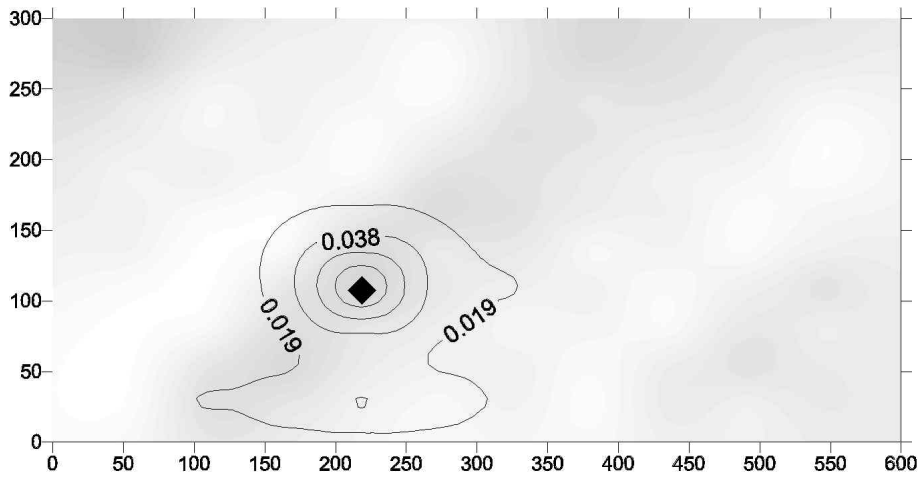


Fig. 10: Normalized error